Optical and Structural Properties of Bismuth Doped ZnO Thin Films by Sol–Gel Method: Urbach Rule as a Function of Crystal Defects

E.F. Keskenler[a,*], S. Aydin[b], G. Turgut[b] and S. Doğan[c]

[a]Recep Tayyip Erdoğan University, Faculty of Engineering, Department of Nanotechnology Engineering Rize, 53100, Turkey

[b]Atatürk University, K. Karabekir Education Faculty, Department of Physics, Erzurum, 25240, Turkey

[c]Department of Electrical and Electronics Engineering, Faculty of Engineering and Architecture Balikesir University, Balikesir, 10145, Turkey

(Received October 3, 2012; revised version April 25, 2014; in final form June 26, 2014)

Bismuth (Bi) doped zinc oxide (ZnO:Bi) thin films were prepared on glass substrates by sol–gel spin coating technique using homogeneous precursor solutions, and effects of Bi doping on the structural and optical properties of ZnO were investigated. The crystalline of ZnO films shifted from polycrystalline nature to amorphous nature with Bi doping. The plane stresses (σ) for hexagonal ZnO and ZnO:Bi crystals were calculated according to the biaxial strain model. The Urbach rule was studied as a function of non-thermal component to the disorder (defects in crystal structures) which is especially observed in the case of non-crystal semiconductors. The calculated Urbach energies and steepness parameters of undoped ZnO and ZnO:Bi films varied between 44.33 meV and 442.67 meV, and 58.3×10^{-2} and 5.8×10^{-2}, respectively. The Urbach energies of the films increased with an increase in the Bi doping concentration and a great difference was observed for 7.0 mol.% doping. The band gap values of the films exhibited a fluctuated behavior as a result of doping effect.

DOI: 10.12693/APhysPolA.126.782

PACS: 78.20.−e, 78.66.Hf, 78.40.Fy, 78.66.Jg, 68.37.Yz, 68.55.ag, 68.60.Bs

1. Introduction

The wide band gap II–VI compound semiconductors have attracted much attention due to their strong nonlinear optical effects and potential applications in areas of optical communication and optical computing [1]. Amongst, ZnO is currently attracting attention for applications to UV light emitters, piezoelectric and acoustic wave transducers, transparent electronics and as a window material for display and solar cells [2]. It has many advantages such as availability in bulk, single-crystal form and larger exciton binding energy (60 meV at room temperature), which is the reason to be used in above applications [3]. It is generally known that a perfect crystal lattice is possible only mathematically, but in fact, it does not exist in real crystals. Defects or imperfections are found in all crystalline solids. The existence of defects usually has a profound effect on the physical properties of a crystal, which is particularly true for semiconductor materials. Therefore, it is important to discuss various types of defects that are commonly observed in a crystalline solid [4].

In 1953, Urbach has studied the optical absorption in AgBr crystal that was the first to show experimentally exponential increase of the absorption coefficient with the incident photon energy. The exponential parts of the absorption edge spectra revealed a typical bundle with the increase of temperature [5, 6]. As shown by Cody et al. [7], besides the thermal component, there is additionally non-thermal component to the disorder, which is clearly manifested especially in the case of amorphous semiconductors [8].

Some properties of ZnO can be changed by doping with different elements like bismuth (Bi). The undoped and Bi doped ZnO (ZnO:Bi) films were deposited by many deposition techniques. Among these, sol–gel spin coating is a useful alternative to the traditional methods for fabricating thin films of ZnO. It is of particular interest because of its low cost, simplicity; and sol–gel process allows the coating of large surfaces and it is useful for industrial production.

In this paper, we have reported the investigation of absorption in Urbach's spectral region of undoped ZnO and ZnO:Bi thin films for several reasons due to a carrier impurity interaction, a carrier–phonon interaction, a structural disorder and etc. at room temperature ($T = 300$ K).

2. Experimental

In the present work, undoped and ZnO:Bi thin films with different Bi concentrations were deposited on microscopic glass substrates by spin coating sol–gel method. When the coating precursor solution was prepared, zinc acetate dehydrate [$Zn(CH_3COO)_2{\cdot}2H_2O$], 2-methoxyethanol ($C_3H_8O_2$), and monoethanolamine (C_2H_7NO, MEA) were used as starting material solvent and stabilizer, respectively. For the BiZO (ZnO:Bi) solution, the bismuth(III) chloride was inserted into the precursor coating solution as the bismuth source. 0.5 M

*corresponding author; e-mail: keskenler@gmail.com, eyupfahri.keskenler@erdogan.edu.tr

zinc acetate dehydrate and 0.5 M bismuth(III) chloride were mixed in different solution atomic percent ratios from 1 at.% to 9 at.% with 2 at.% steps. The molar ratios of all metal ions to MEA were maintained at 1:1. The sol solutions were stirred at 80 °C for 12 h to obtain a clear and homogeneous solution. The glass substrates firstly were kept in boiling chromic acid solution and then they were rinsed with deionized water. Finally, they were cleaned with acetone, deionized water, and methanol by using an ultrasonic cleaner and dried with nitrogen.

In the spin coating process, the resultant solutions were dropped on glass substrate, which was rotated at a speed of 1500 rpm for 25 s by using a spin-coater. The as--coated film was sintered at 200 °C for 5 min to evaporate solvent and remove the organic sediments and then spontaneously cooled to room temperature. This procedure was repeated for 10 times to obtain the intended thickness and film quality. The same procedure was repeated for the films prepared with different values of bismuth doped and finally they were annealed in air at 450 °C for 30 min.

X-ray diffraction (XRD) patterns were taken using a Rigaku Miniflex II diffractometer. The diffractometer reflections were investigated at room temperature and the values of 2θ were altered between 20° and 90°. The incident wavelength was 1.5406 Å. The optical transmittance of the thin films were recorded in spectral region of 300–1000 nm at 300 K using a UV-VIS spectrophotometer (Perkin-Elmer, Lambda 35) which works in the range of 200–1100 nm and has a wavelength accuracy of better than ±0.3 nm. The controlled spin coating technique which is often leading to colloid particles with narrow size distributions to deposit ZnO thin films, has been used. The scope of the present study is to investigate the Urbach rules at ZnO thin films as a function of disorders (occurred by Bi doping) in crystal structures.

3. Result and discussion

The crystal structures of the ZnO and ZnO:Bi films were analyzed by XRD method. XRD spectra of all the films were measured at room temperature. Figure 1 shows the XRD patterns of the undoped and ZnO:Bi films. As seen in Fig. 1, all the peaks of the XRD patterns are indexed to ZnO with the hexagonal wurtzite structure (zincite phase) [9] and with the Miller indices of the peaks given belong to the ZnO [10]. Metallic zinc or bismuth characteristic peaks were not observed from the XRD patterns. The presence of structural peaks in these XRD patterns confirmed the polycrystalline nature of the films. As shown in Fig. 1, undoped thin film has (002) preferred orientation [11] and 1.0 mol.% doped ZnO:Bi film has (100) and (101) peaks in addition to (002) peak. The other films do not show any preferential orientation of crystallization because of having almost the same peaks which are at noise level with relatively low intensity.

The crystalline structure of the films has been deteriorated with Bi doping. The undoped ZnO film which has relatively single-crystalline nature shifted to polycrystalline nature for 1.0 mol.% Bi doped ZnO film and

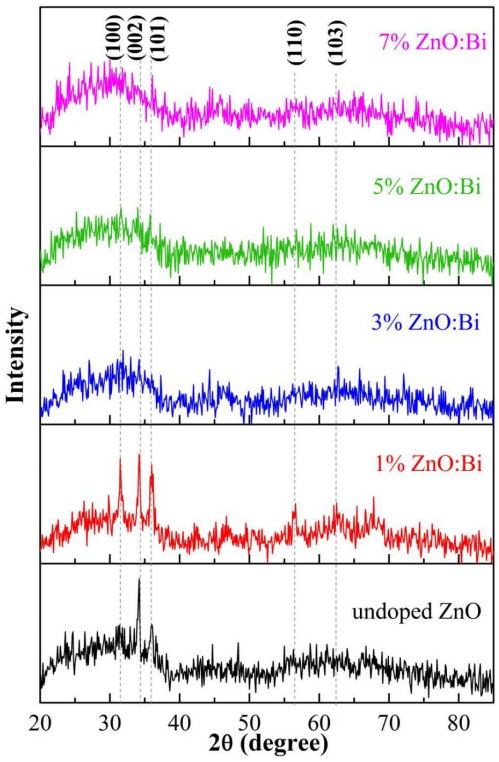

Fig. 1. X-ray diffraction spectra of the ZnO and ZnO:Bi films.

amorphous nature for the other doping contents. The intensity of the (100) and (101) peaks have been fluctuated with increasing the Bi doping content that they were firstly increased to further intensity and then decreased to lower levels. The (002) peak has not been noticeably changed for 1.0 mol.% Bi doping compared to undoped ZnO. But in further Bi doping concentrations, it has not been visible like the others. This is the fact that ZnO:Bi films do not have a good crystallization. The crystallite size was calculated for two films using Scherrer's formula. The Debye–Scherrer approach based on the X-ray line broadening was performed for an approximation of the average crystal size, using the Debye–Scherrer equation [8]:

$$D = \frac{4}{3}\frac{0.9\lambda}{\beta\cos\theta}, \tag{1}$$

where D is the average diameter of the crystals (in spherical approximation), $\lambda\,(=1.5406$ Å) is the wavelength of used X-ray radiation, β is the full width at half maximum (FWHM) intensity of the peak which is the broadening of diffraction line measured at half its maximum intensity in radians and θ is the angle of diffraction corresponding to its maximum. The calculated average values for undoped and 1.0 mol.% ZnO:Bi films were found to be 34.1 and 50.2 nm, respectively. The average crystal size of the other films could not be calculated due to the absence of the peaks for using calculation of FWHM.

According to XRD results the crystalline of the ZnO film is deteriorated with Bi incorporation. The grain

size of crystallite of the films is changed depending on the difference in the ion radii (Zn^{2+} $r = 88$ pm and Bi^{3+} $r = 117$ pm with $1d = 100$ pm) of the dopant element. Incorporation of Bi^{3+} in the ZnO crystal structure can cause reducing the crystallization and increasing the stress in crystal and hence the crystalline structure shifts the amorphous as a result of ion radii difference between the Zn^{2+} and Bi^{3+}.

TABLE I

Standard and calculated interplanar distances d values of the undoped ZnO and 1% ZnO:Bi films.

(hkl)	Standard d [Å]	Observed d [Å]	
		undoped ZnO	1 mol.% ZnO:Bi
100	2.814	2.851	2.842
002	2.603	2.615	2.621
101	2.475	2.492	2.496

The calculated interplanar distance d values from XRD studies by using the Bragg law for undoped and 1.0 mol.% ZnO:Bi films are presented in Table I. These values were also compared with the standard ones from JPCDS card no. 36-1451. The matching of the calculated and standard d values confirms that the deposited films are of ZnO with a hexagonal wurtzite structure. Also, the lattice constants a and c of the wurtzite structure of ZnO can be calculated using the relations given below;

$$\frac{1}{d^2} = \frac{4}{3}\left(\frac{h^2+k^2+hk}{a^2}\right) + \left(\frac{l^2}{c^2}\right). \tag{2}$$

in which d is the interplanar distance and (hkl) Miller indices, respectively. The standard and calculated lattice constants are given in Table II. The calculated a and c values agree with JPCDS card no. 36-1451. Plane stress (σ) of hexagonal crystals with a highly c-axis preferred orientation was calculated according to the biaxial strain model [12]:

$$\sigma = \left[2C_{13} - C_{33}\left(C_{11}+C_{12}\right)/C_{13}\right](c-c_0)/c_0, \tag{3}$$

where c_0 is the corresponding bulk value (5.207 Å), c is the lattice parameter obtained from the (002) diffraction in the XRD, and C_{ij} are elastic stiffness constants ($C_{11} = 2.1 \times 10^{11}$, $C_{12} = 2.1 \times 10^{11}$, $C_{13} = 2.1 \times 10^{11}$, and $C_{33} = 2.1 \times 10^{11}$ N/m^2). The stress can be obtained by the following simplified relation:

$$\sigma = -4.2 \times 10^{11}(c-c_0)/c_0 \text{ [N/m}^2\text{]}. \tag{4}$$

The calculated results are listed in Table II. The compressive stress on the films was indicated by the negative sign. The total stresses in the film collectively depend on both intrinsic and extrinsic stresses which occur by defects and impurities in the crystal by the lattice mismatch between the film and substrate, respectively. As can be seen in Table II, the Bi incorporation in the structure has increased the strains in the film.

TABLE II

Various optical and structural parameters of undoped ZnO and ZnO:Bi thin films.

Bi ratio [mol.%]	Urbach energy (E_u) [meV]	Band gap [eV]	Steepness parameter (σ)	Lattice constants [Å]*		D [nm]	Stress [N/m^2]
				a	c		
0	44.33	3.28	58.3×10^{-2}	3.282	5.231	34.109	-1.94×10^9
1	64.28	3.25	40.2×10^{-2}	3.392	5.242	50.236	-2.82×10^9
3	66.18	3.31	39.1×10^{-2}	–	–	–	–
5	92.46	3.31	28.0×10^{-2}	–	–	–	–
7	442.67	3.17	5.8×10^{-2}	–	–	–	–

$a^* = 3.250$ Å, $c^* = 5.207$ Å (* JPCDS card no: 36-1451, standard a and c values)

In the literature, there is a remarkable interest in existence of exponential absorption tails for photon energies of sub-band gap of both crystalline and amorphous materials. Although various mechanisms can affect the absorption phenomena in principle, it seems that excitons have a significant role. The optical absorption coefficient of a semiconductor shows a temperature-dependent exponential tail for the range of energies $E < E_g$ [13]:

$$\alpha(E,T) = \alpha_0 \exp\left(\frac{E-E_0}{E_u(T,X)}\right). \tag{5}$$

In this equation, E_0 and α_0 are constants, which can be determined from the $\ln(\alpha)$ versus E obtained at series of different temperatures. E_0 almost overlaps at zero lattice temperature with the energy of the lowest free exciton state. The E_u is the Urbach energy which is assigned the steepness of Urbach tail. It is a function of temperature (T) and the degree of crystal disorder (X) of the material; and it has also a significant role on the characteristic analysis of a studied semiconductor. The dependence of E_u on temperature model suggested by Cody can be expressed with the following equation [6, 7, 14]:

$$\sigma(T) = \sigma_0 \left(\frac{2kT}{\frac{h}{2\pi}\omega_p}\right) \tanh\left(\frac{\frac{h}{2\pi}\omega_p}{2kT}\right). \tag{6}$$

σ_0 is a material-dependent but temperature-independent parameter that is inversely proportional to the strength of the coupling between phonons and excitons. $h\omega_p$ corresponds to the energy of phonons related with the Urbach tail. The parameter σ/kT for the interaction between

exciton and longitudinal-optical (LO) phonons coincides with Eq. (6) by a constant factor [15].

As shown by Cody et al. [7] besides the thermal component to the structural disorder mechanism, there is an additional non-thermal component to the disorder (defects in crystal structures), which is clearly observed especially in the case of non-crystal semiconductors. This contribution is expected to exhibit a temperature-independent component to the Urbach exponential absorption edge. The previous statements imply that the Urbach energy can be expressed as two components; temperature--dependent and temperature-independent term:

$$E_{\mathrm{u}}(T,X) = E_{\mathrm{u}}(T) + E_{\mathrm{u}}(X). \tag{7}$$

The thermal disorder of the material is associated with the temperature-dependent term, while the temperature--independent component related to its inherent structural disorder [13]. If the width of the edge is related to the slope of Eq. (6), the σ parameter is found as

$$\sigma = kT/E_{\mathrm{u}}. \tag{8}$$

By taking the natural logarithm on both sides of Eq. (5):

$$\ln\alpha = E\frac{1}{E_{\mathrm{u}}}\left(\ln(\alpha_0) + \frac{E_0}{E_{\mathrm{u}}}\right). \tag{9}$$

E_{u} is equal to the absorption edge energy width and inverse to the absorption edge slope value $E_{\mathrm{u}}^{-1} = \Delta(\ln\alpha)/\Delta(h\nu)$. E_{u} should depend only on the degree of structural disorders (lattice strains and dislocation densities), i.e. as a function of X, in a constant temperature. In the present study, we have investigated the E_{u} as a function of disorder on the non-crystalline structures by depositing amorphous thin film material.

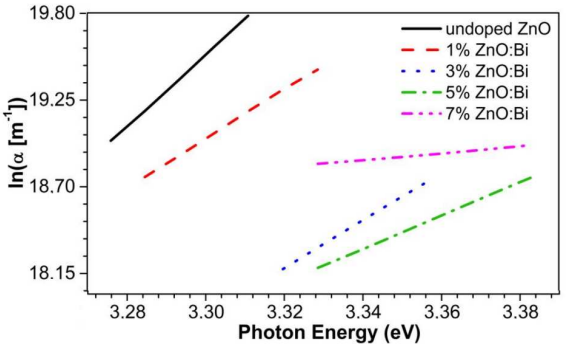

Fig. 2. Spectral dependences of logarithm of absorption coefficient for ZnO and ZnO:Bi films as a function of defects (Urbach plots).

The plots of $\ln\alpha$ versus photon energy for undoped and ZnO:Bi thin films at 1.0%, 3.0%, 5.0%, and 7.0 mol.% are given in Fig. 2. This treatment can correspond primarily to optical transitions between occupied states in the valence band tail to unoccupied states at the conduction band edge [16]. The obtained E_{u} values are given in Table II. The Urbach energy values of the films increase with Bi incorporation. The optical band gaps of the films change reversely with the Urbach energy values. This result causes a redistribution of states, such as from band to tail and tail to tail transitions [17] and in turn, the optical gap decreases due to the broadening of the Urbach tail. These results obtained for Bi doped ZnO are in agreement with the findings obtained for other kind of impurities, such as Sn, F, Al, Er, Ta, In [16]. It can be seen that Bi incorporation into ZnO causes a significant increase in the Urbach energy, compared to ZnO films, as a result of increasing structural disorder, by confirmed XRD spectra. The steepness parameters of the films were calculated by using Eq. (8) at $T = 300$ K and are given in Table II. The variation of σ values suggests that Bi incorporation affected the absorption edge. The fact that σ value of the undoped ZnO film is higher than that of ZnO:Bi film can be expressed as broadening of the absorption edge. The optical absorption theory gives the relationship between the absorption coefficients (α) and the photon energy ($h\nu$) for the direct transition. The optical band gap values can be calculated by the following relation [18]:

$$(\alpha h\nu) = A\left(h\nu - E_{\mathrm{g}}\right)^n, \tag{10}$$

where α is the absorption coefficient, $h\nu$ — the photon energy, A is a constant, and E_{g} is the optical band gap. n is an index that characterizes the optical absorption and it is equal to 2 and 1/2 for indirect and direct allowed transitions, respectively. The relationship of absorption coefficient on photon energy exposes detailed information about the energy band gaps. It can be seen from Fig. 3 that the plots of $(\alpha h\nu)^2$ versus photon energy for the films. The optical band gap values of the films were determined from extrapolation of the dashed straight lines to $\alpha^2 = 0$ and are given in Table II. Firstly, E_{g} value of the ZnO film decreased with Bi incorporation, after an increase was observed above the undoped ZnO value and finally it decreased to the lowest value. As a result, there is a great difference between undoped and 7.0 mol.% Bi doped ZnO films, which is attributed to the shrinkage effect of the optical band gap. The optical band gap fluctuation due to the broadening of valence and conduction bands is related to interactions among d, s, and p electrons of Bi and host atoms, respectively.

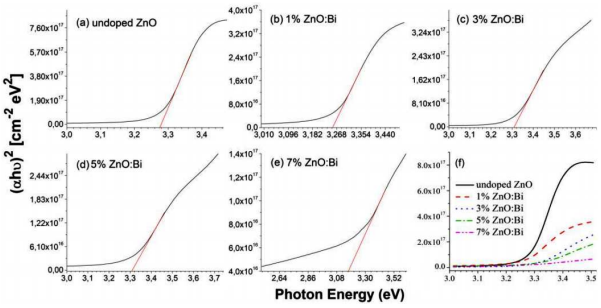

Fig. 3. Plot of $(\alpha h\nu)^2$ versus photon energy for ZnO and ZnO:Bi thin films.

Optical transmission spectra of ZnO:Bi and undoped ZnO films were recorded in the wavelength range 300–1000 nm and are given in Fig. 4. The transmission spectra do not show interference fringes. The invisibility of interference fringes indicates rough surfaces mean-

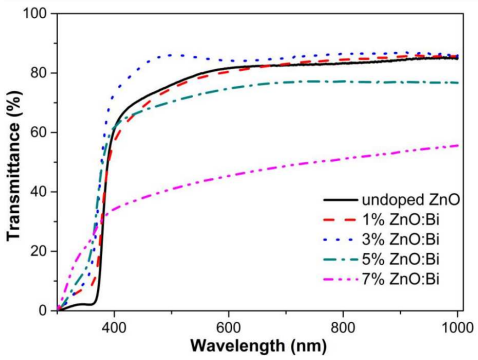

Fig. 4. Optical transmittance spectra of undoped and various Bi doped ZnO films.

ing granular reflecting surface of the films and maximum scattering loss, which is indirectly related to the doping effects. The undoped film exhibits about 70% transmittance, when Bi was incorporated into the ZnO films, a decrease was observed after sharp increase to 80–85% in transmittance at about 350 nm for 3.0 mol.% Bi doped ZnO. In the last, a great decrease was observed to 35% for 7.0 mol.% Bi doped ZnO film. The increase in transmission spectra at the edge of UV region can be due to increase in zinc sites occupied by Bi which is related to increase in carrier concentration, commonly known as the Burstein–Moss effect [19]. This result can be attributed to the increase of electron carrier concentration with the substitution of Bi^{3+} ions to Zn^{2+} ions.

As shown in Fig. 4, 7.0 mol.% Bi doped ZnO shows great difference, compared to undoped ZnO, it has new absorption edges, which indicates that some trapping states have been formed with Bi doping, and introduces new electronic states into the band of ZnO to form a new lowest unoccupied molecular orbital (interband trap site) [20].

4. Conclusion

Undoped and ZnO:Bi films were successfully prepared by sol–gel spin coating technique and effects of Bi doping on optical and structural properties of the ZnO were investigated. The crystal structure of ZnO shifted to amorphous nature with Bi doping and the Urbach rule was studied on these films as a function of crystal defects. The Urbach rule being revealed in the absorption spectra of non-crystalline solids were considered as well as the effect of non-thermal disordering processes on the optical absorption edge parameters. The Urbach energy values of the films increased with Bi incorporation. This result was attributed to sub-band gaps. The optical band gaps of the films changed reversely with the Urbach energy values.

The stress values of ZnO crystal film increased with the increasing Bi concentration. From the optical transmission spectra, the undoped film had high transmittance about 70%. When Bi was incorporated in ZnO with 1.0 mol.% Bi content, a decrease in optical transmittance was observed, after it sharply increased about 80–85% at around 350 nm for 3.0 mol.% Bi doped ZnO. Finally, a great decrease was observed up to the value of 35% for 7.0 mol.% Bi doped ZnO film. These results shows that Bi doped ZnO can be a good candidate for amorphous applications.

References

[1] D. Behera, B.S. Acharya, *J. Lumin.* **128**, 1577 (2008).

[2] S. Kim, B.S. Kang, F. Ren, K. Ip, Y.W. Heo, D.P. Norton, S.J. Pearton, *Appl. Phys. Lett.* **84**, 1698 (2004).

[3] Ü. Özgür, Y.I. Alivov, C. Liu, A. Teke, M.A. Reshchikov, S. Doğan, V. Avrutin, S.-J. Cho, H. Morkoç, *J. Appl. Phys.* **98**, 041301 (2005).

[4] S.L. Sheng, *Semiconductor Physical Electronics*, 2nd ed., Springer Science-Business Media LLC, New York 2006.

[5] F. Urbach, *Phys. Rev.* **92**, 1324 (1953).

[6] M. Kranjčec, I.P. Studenyak, M.V. Kurik, *J. Non-Cryst. Solids* **355**, 54 (2009).

[7] G.D. Cody, T. Tiedje, B. Abeles, B. Brooks, Y. Goldstein, *Phys. Rev. Lett.* **47**, 1480 (1981).

[8] M.T. Weller, *Inorganic Materials Chemistry*, Oxford University Press, Oxford 1997.

[9] T. Wang, Y. Liu, Q. Fang, M. Wu, X. Sun, F. Lu, *Appl. Surf. Sci.* **257**, 2341 (2011).

[10] Joint Committee on Powder Diffraction Standards (Powder Diffraction File, card no: 36-1451).

[11] Y. Caglar, S. Ilican, M. Caglar, F. Yakuphanoglu, *Spectrochim. Acta A* **67**, 1113 (2007).

[12] S. Maniv, W.D. Westwood, E. Colombini, *J. Vac. Sci. Technol.* **20**, 162 (1982).

[13] E.A. Meulenkamp, *J. Phys. Chem. B* **103**, 7831 (1999).

[14] S. John, C. Soukoulis, M.H. Cohen, E.N. Economou, *Phys. Rev. Lett.* **57**, 1777 (1986).

[15] H.W. Martienssen, *J. Phys. Chem. Solids* **2**, 257 (1957).

[16] Y. Caglar, S. Ilican, M. Caglar, F. Yakuphanoglu, *J. Sol-Gel Sci. Technol.* **53**, 372 (2010).

[17] S.K. O'Leary, S. Zukotynski, J.M.J. Perz, *Non-Cryst. Solids* **210**, 249 (1997).

[18] J. Tauc, *Amorphous and Liquid Semiconductors*, Plenum Press, New York 1974.

[19] B.N. Pawar, D.-H. Ham, R.S. Mane, T. Ganesh, B.-W. Cho, S.-H. Han, *Appl. Surf. Sci.* **254**, 6294 (2008).

[20] J.B. Zhong, J.Z. Li, Y.H. Lu, X.Y. He, J. Zeng, W. Hu, Y.C. Shen, *Appl. Surf. Sci.* **258**, 4929 (2010).